Proteomic identification of activin receptor-like kinase-1 as a differentially expressed protein during hyaloid vascular system regression

Elena Albè, Elizabeth Escalona, Rama Rajagopal, Joel A. Javier, Jin-Hong Chang, Dimitri T. Azar*

Department of Ophthalmology, Harvard Medical School, 243 Charles Street, Boston, MA 02114, USA
Corneal and Refractive Surgery, Massachusetts Eye and Ear Infirmary, 243 Charles Street, Boston, MA 02114, USA
Schepens Eye Research Institute, 20 Staniford Street, Boston, MA 02114, USA

Received 10 August 2005; accepted 15 August 2005

Available online 28 September 2005

Edited by Veli-Pekka Lehto

Abstract The hyaloid vascular system (HVS) is a transient network of capillaries that nourishes the embryonic lens and the primary vitreous of the developing eye. We used proteomic analysis and immunohistochemical staining to identify activin receptor-like kinase-1 (ALK1), a type I receptor for transforming growth factor-β1, during the HVS regression phase. In addition, we overexpressed ALK1 in corneas implanted with bFGF (basic fibroblast growth factor) pellets and observed that ALK1 overexpression resulted in inhibition of bFGF-induced corneal neovascularization in vivo. Our data suggest that ALK1 may play a role in HVS regression during ocular development.

Keywords: Activin receptor-like kinase-1; Hyaloid vascular system regression

1. Introduction

The hyaloid vascular system (HVS) is a transient network of vessels, which traverses the primary vitreous and surrounds the immature lens of the developing eye. The hyaloid artery extends from the optic nerve to the embryonic lens, giving rise to a capillary plexus that surrounds the lens consisting of the vasa hyaloidea propria (VHP), the tunica vasculosa lentis (TVL), and the pupillary membrane (PM). Failure of the HVS to regress in humans can lead to persistent hyperplastic primary vitreous, which, if untreated, can result in blindness.

The precise mechanisms of the regression of the HVS are still unclear. Possible mechanisms include apoptosis of the vascular and endothelial cells [1,2], vitreous-derived regression of the TVL [3–8], macrophage-associated regression of the TVL [9] and hyalocyte-associated transforming growth factor-β (TGF-β) [10].

TGF-β is a potent inhibitor of vascular endothelial cell proliferation [10]. It regulates endothelial proliferation via two receptor/Smad (mother against decapentaplegic) pathways. After ligand binding and activation of Type I receptors, signals are transduced from the membrane to the nucleus via Smads [11]. Type I receptors recruit and phosphorylate Smads, such as Smads2 and 3 by the TβRI/ALK5 type I receptor in response to TGF-β, and Smads1, 5, and 8 by the bone morphogenetic protein type I receptors [12]. Activin receptor-like kinase-1 (ALK1) activates Smads1, 5, and 8, which downregulate VEGF production. In contrast, ALK5 activates Smads2 and 3, which upregulate VEGF production [13]. Expression of ALK1 in blood vessels and mutations of the ALK1 gene in patients with human type II hereditary hemorrhagic telangiectasia, a multi-systemic vascular dysplasia, suggests that ALK1 may play an important role during normal vascular development [14].

We used a proteomic approach to investigate the protein expression and to identify the specific protein changes associated with the regression of the HVS. Two-dimensional electrophoresis and mass spectrometry of the developing mouse lens and vitreous identified ALK1 as a differentially expressed protein during HVS regression; immunohistochemical staining demonstrated the localization of ALK1 in the TVL; and overexpression of ALK1 in the cornea resulted in inhibition of basic fibroblast growth factor (bFGF)-induced corneal neovascularization in vivo.

2. Materials and methods

2.1. Mouse anterior tissue preparation for 2-DE gels

For the protein extraction and ALK1 immunolocalization studies, newborn mice were sacrificed on post-natal days 1, 4, and 16. Using a dry ice bed, frozen mouse eyes were scraped with a blade (Beaver #15) to remove the cornea, conjunctiva, sclera, ciliary body, uvea, and retina, leaving the lens surrounded by the PM, TVL, and primary vitreous (containing VHP). The dry ice bed was used to prevent warming of the specimen, tissue melting and subsequent protein denaturation. Samples of P1, P4, and P16 were pooled and independently solubilized in 250 μl of total protein extraction buffer 7 M urea, 2 M thiourea, 1% (w/v) ASB-14 detergent, 40 mM Tris base, 0.001% bromophenol blue, 20% carrier ampholyte (Biorad Laboratories, Hercules, CA), and 2 μl of 200 mM tributylphosphine by mechanically homogenizing them with an electrical tissue homogenizer for 5 min on ice. The homogenates of the protein extracts were cleared by centrifugation for 20 min at 14000 rpm and 4 °C to remove particulates. Protein concentration of the supernatants was determined by protein assay (Biorad Laboratories). All experiments using animals were conducted in accordance with the Animal Care and Use Committee guidelines of the Massachusetts Eye and Ear Infirmary and the Association for Research in Vision and Ophthalmology (ARVO) Statement for the Use of Animals in Ophthalmic and Vision Research.

*Corresponding author. Fax: +1 617 573 4300.
E-mail address: dazar@meei.harvard.edu (D.T. Azar).

0014-5793/$30.00
doi:10.1016/j.febslet.2005.08.078

2.2. Two-dimensional electrophoresis, image analysis, and protein identification

Three samples per post-gestational day were loaded onto non-linear, immobilized pH gradient (IPG) gel strips (7 cm, pH 3–10), subjected to isoelectric focusing with a programmed voltage gradient at 8000 V for 5 h, and rehydrated overnight with rehydration/sample buffer (Biorad Laboratories). IPG strips were equilibrated with buffer containing 6 M urea, 50 mM Tris (pH 8.8), 30% glycerol, 2% SDS (sodium dodecyl sulfate), and 0.001% bromophenol blue containing 2% dithiothreitol or 2.5% iodoacetamide. Following equilibration, second-dimension separation was performed on 4–20% SDS–PAGE (SDS–polyacrylamide gel electrophoresis gels) (Biorad Laboratories) with the first-dimension IPG strip embedded in 0.5% agarose at the top. After electrophoresis, the proteins on the gel were fixed in 10% acetic acid and 20% methanol for 1 h and then stained with SYPRO Rubin (Biorad Laboratories). Images of the 2-DE (two-dimensional electrophoresis) gels were captured with Molecular Imager FX Pro Plus multi-imager system and the protein expression profiles at each time point were compared, in triplicate, using the Phoretix 2D image analysis software. Protein spots present in P16 with expression level 2- to 10-fold greater than P1 were considered for protein identification. The statistical significance of changes was evaluated using Phoretix 2D software.

Gel bands (differentially expressed proteins) from 2-DE gels were excised, minced into approximate 1 mm^3 pieces with a sterile razor blade of the Xcise technology platform from the Proteome system, alkylated, and digested with trypsin (Promega, Madison, WI). Peptides were resuspended in 50% acetonitrile with 1% formic acid solution and subjected to nano-LC ESI IT MS/MS analysis. A Surveyor LC pump (Thermo Electron, San Jose, CA) with a C18 trapping column (300 μm i.d. × 1 mm, Dionex, Sunnyvale, CA) and a reversed-phase column 75 μm i.d. × 15 cm (Magic C18AQ, 3 μm) was used for nano-LC experiments. An LCQ Deca XP plus ESI mass spectrometer (Thermo Electron, San Jose, CA) was used for all the experiments.

MS/MS data-dependent acquisition followed by database searching with SEQUEST (BioWorks 3.1, Thermo Electron, San Jose, CA) allowed protein identification. Fully tryptic peptides were matched with SEQUEST at a delta correlation (ÄCn) of greater than 0.08 and correlation (Xcorr) greater than 1.9, 2.2, and 3.5 for charged states of +1, +2, and +3, respectively. Peptide mass fingerprints were searched for matches with the virtually generated tryptic protein masses of the NCBInr mouse protein sequence database (www.ncbi.nml.nih.gov). All databases were provided in the public domain by the host institutions. Proteins were noted as differentially expressed if they could not be located at the corresponding position on the 2-DE gel of the other time point.

2.3. ALK1 immunolocalization by confocal microscopy

Mouse eyes harvested at P1, P4, and P16 were embedded in optimal cutting temperature compound (Miles, Elkhart, IN), frozen in liquid nitrogen, cryostat sectioned, and fixed in acetone for 10 min. After blocking with 1% bovine serum albumin (BSA) (Sigma Chemical Co., St. Louis, MO) for 30 min, the sections were incubated for 1 h with rabbit anti-ALK1 polyclonal antibody (courtesy of Dr. D.A. Marchuck, University of North Carolina) at a concentration of 1:200. A secondary antibody used was fluorescein-conjugated, affinity-purified anti-rabbit IgG antibody (Jackson ImmunoResearch Laboratories, West Grove, PA) at a concentration of 1:400. Negative controls were prepared in the same manner, with 1% BSA without primary antibody. Immunostained sections were viewed with a Leica TCS SP2 CLSM confocal laser scanning microscope (Leica, Heidelberg, Germany).

2.4. Plasmid construction and corneal naked DNA injection

pYX-Asc-ALK1 cDNA was purchased from ATCC (Manassas, VA). Plasmids were purified using a Qiagen kit (Valencia, CA) according to the manufacturer's instructions. The mouse ALK1 DNA was sequenced and subcloned into pEF expression vector. An Elongation Factor 1 alpha promoter (pEF) was used to drive the expression of the ALK1 gene. Mouse corneas received a DNA injection of 5 μl of pEF-ALK1 (400 ng/μl) or an injection of 5 μl of vector (400 ng/μl). An antibiotic ophthalmic ointment was used after surgery.

2.5. bFGF pellet preparation and corneal micropocket assay

Pellets were made of the slow-release polymer Hydron (polyhydroxyethylmethacrylate), which contained a combination of 45 ng/pellet of sucralfate (Sigma) and 120 ng/pellet of bFGF (R&D Systems, Minneapolis, MN) as previously described by Kenyon et al. [15].

Briefly, a suspension of sterile saline containing the appropriate amount of recombinant bFGF and sucralfate was made and speed-vacuumed for 8 min. To this suspension, 10 μl of 12% Hydron in ethanol was added. The suspension was then deposited onto a sterilized nylon mesh (LAB Pak, Sefar America, Depew, NY) and embedded between the fibers. The resulting grid of 10 mm × 10 mm squares was allowed to dry on a sterile Petri dish for 60 min. The fibers of the mesh were pulled apart under a microscope and, among the approximately 100 pellets produced, 30–40 uniformly-sized pellets of 0.4 × 0.4 × 0.2 mm were selected for implantation. All procedures were performed under sterile conditions.

Three days after the naked DNA injections, corneal micropockets were created with a modified von Graefe knife in C57BL/6 mice. Hydron pellets containing 120 ng of human bFGF were implanted into the corneal pockets.

2.6. Measurement of corneal neovascularization

The corneas were routinely examined and photographed in five positions: en face, superior, inferior, nasal, and temporal with a slit lamp biomicroscope (Nikon FS-2, Tokyo, Japan) on days 1, 4, 7, and 14 post-pellet implantation. The photographs were digitized and the images were resolved at 300 pixels/in. and analyzed with the NIH ImageJ image program (NIH, Bethesda, MD). NIH ImageJ program was used to calculate the area of corneal neovascularization areas. Statistical analysis was performed with the Student *t*-test.

3. Results

3.1. Progressive regression of HVS in the mouse and the differential protein expression profile

We designed a time course experiment to examine the changes in protein expression at P1 and P16 throughout the HVS regression process. As this is the first reported application of proteomic analysis on HVS regression, several conditions for tissue selection and preparation were developed and optimized to obtain clean specimens of the lens and vitreous for 2-DE gels.

We generated protein expression maps in triplicate for each time point, obtaining a reproducible separation of the protein spots on the 2-DE gels. We could detect up to 1400 protein spots in each gel with the Phoretix 2D image analysis software (Fig. 1A). This software allows the possibility to warp different gel images to improve the quality of the protein spot matching between the gels and allow an easy detection of the differences among the gels. We analyzed our 2-DE gels and observed a progressive decrease in the number and intensity of the protein spots from P1 to P16, particularly of the migrated proteins in the area corresponding to p*I* 4–7 and M_w 30–90 kDa (Fig. 1B–C).

However, the warping of the 2-D gel images of P1 with P16 revealed the presence of a small number of protein spots for which expression level in P16 was 2- to 10-fold greater than P1. 20 protein spots were analyzed using mass spectrometry analysis. Some of these identified proteins displayed slightly different molecular weights and p*I*s, suggesting the presence of different isoforms or post-translational modifications. Eighteen differentially expressed proteins were identified, two additional proteins were unclassified, and fifteen were unknown. ALK1 was identified as spot #17.

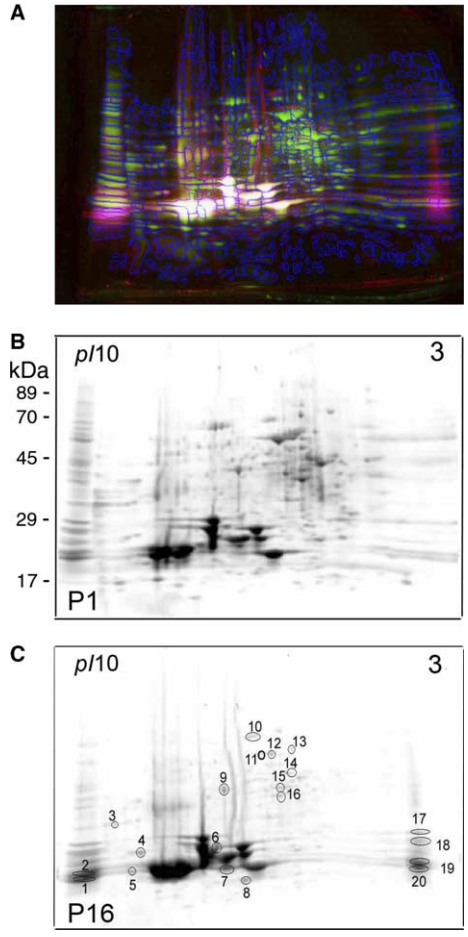

Fig. 1. Proteomic analysis of proteins from the lens and vitreous of P1 and P16 mice. The merged image (A) represents the warped image between P1 (B) and P16 (C) obtained with Phoretix 2D evolution software. The proteins excised from 2-D gel (P16) for analysis and identification by mass spectrometry are identified with numbers 1–20 (C).

3.2. Immunolocalization of ALK1 in the TVL by confocal microscopy

To investigate whether ALK1 is expressed in TVL during mouse development, mouse eyes at P1, P4 and P16 were immunostained with anti-ALK1 antibody. The confocal immunohistochemical staining demonstrated that ALK1 is localized in the endothelial cells of the TVL at P1, P4, and P16 (Fig. 2A, C and E).

3.3. Naked DNA, pEF-ALK1, blocked bFGF-induced corneal NV

Naked DNA has been effectively used for the delivery of DNA into mouse corneas. To assay if ALK1 can inhibit bFGF-induced corneal NV (neovascularization), mouse corneas were injected with naked DNAs of pEF (vector) and pEF-ALK1. The ALK1 plus pellet group (Fig. 3M–P) showed no evidence of corneal NV at any time point after pellet implantation. The group receiving vector control plus pellets (Fig. 3I–L) began to develop corneal NV at day 4, and the new vessels continued to grow toward the pellet area at days 7 and 14. The area occupied by NV in the ALK1 treated mice was 0.58 and 0.47 mm^2 at days 7 and 14 after bFGF pellet implantation, respectively (Fig. 3O–P). This was significantly less than the NV areas in vector treated mice, which were 3.14 mm^2 ($p = 0.001$) and 3.33 mm^2 ($p = 0.001$) at 7 and 14 days after bFGF pellet implantation, respectively (Fig. 3K–L). The no-pellet control groups [ALK1 naked DNA (Fig. 3E–H) and vector naked DNA (Fig. 3A–D)] did not induce corneal NV.

4. Discussion

Genetic studies in mice and humans have demonstrated that the TGF-β signaling pathway plays an important role in the maintenance of vascular homeostasis during embryogenesis and during adult life [16]. Depending on the experimental conditions, TGF-β may act as an inhibitor or a stimulator of angiogenesis in vitro and in vivo [17,18]. However, the molecular mechanisms and target cells by which the pleiotropic TGF-β elicits its pro- and anti-angiogenic properties remain unclear [13].

ALK1 is one of the seven Type I receptors for the TGF-β family of proteins [19]. Its expression has been detected in endothelial cells of highly vascularized tissues (lungs and placenta) [20], normal and neoplastic pituitary cells [21], anaplastic large

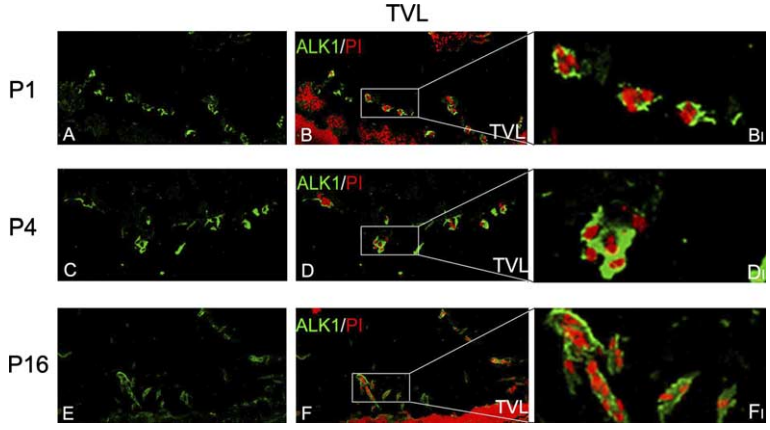

Fig. 2. Confocal immunohistochemical localization of ALK1 in the mouse eye during development. Mouse eyes at postnatal days 1, 4 and 16 were sectioned. Sections of the tunica vasculosa lentis at P1, P4 and P16 were immunostained with anti-ALK1 antibodies (A,C,E) and PI staining, and the resulting images were merged (B,D,F). The TVL areas are enlarged in Fig. 2 B_1, D_1 and F_1.

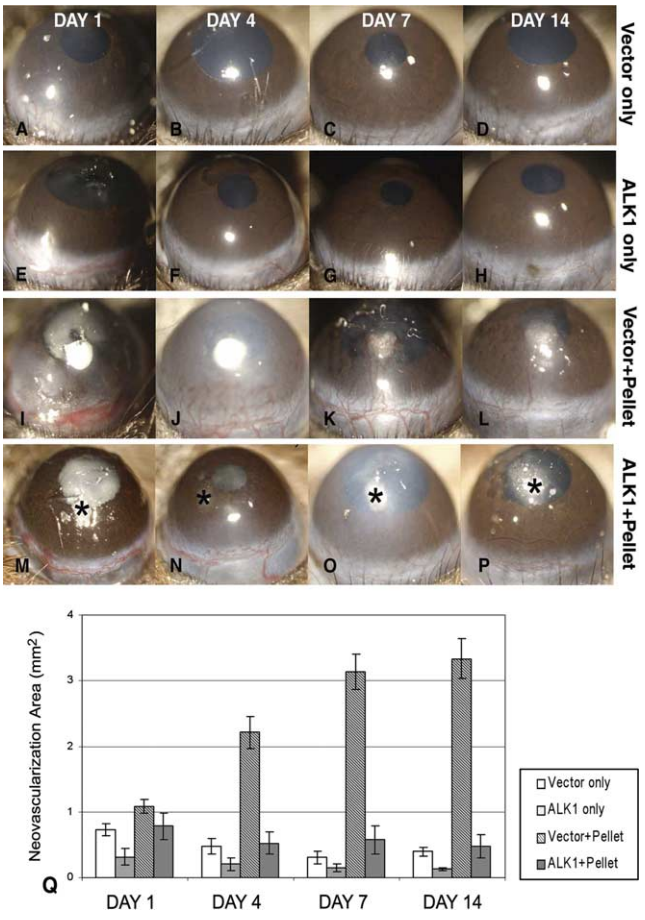

Fig. 3. bFGF-induced corneal NV is inhibited by naked ALK1 DNA injection in vivo. No-pellet controls are shown in A–H: Injection of naked DNA [ALK1 (E–H) and vector only (A–D)] did not induce corneal NV. The vector plus pellet positive controls are shown in I–L: Development of NV in the corneal stroma was evident by day 4 (J); new vessels continued to grow in the direction of the pellet on days 7 and 14. None of the mice in the ALK1 and pellet groups (M–P) showed development of corneal NV on days 1, 4, 7, and 14 after pellet implantation. Asterisk (*) indicates pellet implantation. The area of corneal NV of the four groups at days 1–14 is shown (Q).

cell lymphoma [22], inflammatory myofibroblastic tumor [23] and central nervous system cells [24]. ALK1 transduces the TGF-β1 signal by phosphorylating Smad1, Smad5, or Smad8 [13,14]. Upon phosphorylation by the receptors, Smad complexes translocate into the nucleus, where they cooperate with sequence-specific transcription factors in the promoter DNA to regulate gene expression [12]. This functional and physical interaction confers both specificity and complexity in transcriptional responses to TGF-β family ligands [12].

Mutations of the ALK1 or endoglin genes have been linked to the human vascular disorder Hereditary Hemorrhagic Telangiectasia (HHT) [25,26]. This is an autosomal-dominant disorder, also known as Osler-Rendu-Weber syndrome, characterized by the age-dependent development of focal arteriovenous malformations and telangiectases [27]. HHT type 2 is caused by loss of function of the activin receptor-like kinase 1 (ACVRL1 or ALK1) [27]. The disease is characterized by dilated, thin-walled, vascular anomalies of the skin and mucous membranes and recurrent epistaxis. In literature, abnormal eye disorders have been documented in 45–65% of patients with HHT, with the most common lesions being conjunctival telangiectasias [28,29]. Retinal arteriovenous malformations, retinal telangiectasia and choroidal haemorrhage during intraocular surgery have also been noted [28,30].

Identification of ALK1 by proteomic analysis and immunohistochemistry in our model of HVS regression is consistent with Lutty's observation that the TGF-β1 pathway may play an important role in the remodeling of ocular vasculature [10]. However, the exact role of ALK1 in angiogenesis remains controversial. Goumans et al. [13] suggested that the constitutively active form of ALK1 promotes endothelial cell migration and proliferation by upregulating Id-1, a transcription factor promoting vascular growth through repression of thrombospondin-1.

Lamouille et al. [31] have suggested that ALK1 is implicated in the maturation phase of angiogenesis. They showed that the transfection of a constitutively active form of ALK1 (which results in a constitutive ligand-independent receptor activation) inhibits both endothelial cell proliferation at the G1 phase of the cell cycle and endothelial cell migration through a modification of the dynamics of the endothelial cell cytoskeleton. Consistent with these results, a zebrafish *ALK1* mutant, *vgb*, whose vessel dilation phenotype is reminiscent of that of the *ALK1*−/− mice, showed an increased number of endothelial cells within the affected vessels, suggesting the role of ALK1 in the inhibition of endothelial cell proliferation [32].

Several studies have reported that ALK1 stimulates the resolution phase of angiogenesis. Oh et al. [14] observed that ALK1 deficient (−/−) embryos die at midgestation and exhibit severe vascular abnormalities characterized by excessive fusion of capillary plexes into cavernous vessels and hyperdilation of large vessels. They suggested that ALK1 plays a role in the inhibition of endothelial cell proliferation and in the stabilization of vessel structural integrity.

In their studies of the ALK1 expression patterns during wound healing, Seki et al. [11] showed that ALK1 was almost undetectable in the numerous capillaries that had formed in the area surrounding the wound. This evidence also supports the role of ALK1 in the resolution phase rather than the activation phase of angiogenesis. The discrepancies between the ascribed roles of ALK1 in different studies may be due to differences in the cell lines and cultures used or possible secondary adaptive processes that may take place in the embryo during development in order to counteract the lack of ALK1 expression [33].

Lebrin et al. [34] clarified these conflicting reports about ALK1 function presenting the activity of endoglin as modulator of the balance between TGF-β1/ALK1 and TGF-β1/ALK5 signaling pathways. They showed how endoglin induces endothelial cell proliferation and migration, promoting an efficient TGF-β1/ALK1 interaction. In the absence of endoglin, endothelial cells do not proliferate and ALK1 signaling is abrogated; unopposed ALK5 signaling maintains the endothelium quiescence [33].

The model of pellet-induced corneal NV used in our experiment is especially advantageous because it is reproducible and it facilitates investigation of angiogenesis in various murine tumor models as well as in genetically defined murine strains [15]. This model has been used to confirm the anti-

angiogenic activity of several anti-angiogenic factors including angiostatin [35], endostatin [36,37], PEDF [38], and neostatin [39]. With this in vivo model, we demonstrated that an overexpression of ALK1 in the mouse cornea (through naked DNA injection) does not induce corneal NV and can prevent the growth of bFGF-induced new stromal vessels. Our results showing the anti-angiogenic activity of ALK1 are of particular interest given its role in HVS regression.

As the hyaloid vessels are arteries, our findings are consistent with those of Seki et al. [11] showing that ALK1 expression is induced in the pre-existing feeding arteries and newly forming arterial vessels in wound healing and tumor angiogenesis, but is greatly diminished in adult arteries, suggesting that the expression of ALK1 may play an important role in the arterialization phase mediating the TGF-β1 signal. Supporting this view, ALK1 KO mice suffer from generalized developmental arrest by E10.5 due to defects in vascular smooth muscle cell differentiation and recruitment [40]. Better understanding of the mechanisms of ALK1 activation may provide the basis for future therapeutic interventions to prevent and treat ocular NV.

Acknowledgments: Supported by the National Institutes of Health [NIH EY10101 (D.T.A.), EY14048 (J.H.C.)], and Research to Prevent Blindness Lew R. Wasserman Merit Award (D.T.A.).

Appendix

Differential protein expression at post-gestational day 16.

SPOT #	Protein Name
1	RAD50 homolog
2	Olfactory receptor GA_x6K02T2PBJ9-6773690-6774628
3	Cofilin 1, non-muscle
4	Guanine nucleotide-binding protein, β-1 subunit
5	Protein kinase, cAMP dependent regulatory, type I β
6	α enolase (2-phospho-D-glycerate hydro-lyase) (non-neural enolase)
7	Cathepsin 3 precursor
8	Unclassified
9	Knsl7 protein
10	F-box/LRR-repeat protein 3B (F-box and leucine-rich repeat protein)
11	Enolase 3, β muscle
12	Albumin 1
13	Heat shock cognate 71 kDa protein
14	Fatty acid binding protein 5, epidermal; keratinocyte lipid binding protein
15	Vimentin
16	Tubulin, β 2
17	ALK1 protein
18	CRAA_MOUSE α crystallin A chain, major component
19	Crystallin, β A4
20	Unclassified

References

[1] Meeson, A., Palmer, M., Calfon, M. and Lang, R. (1996) A relationship between apoptosis and flow during programmed capillary regression is revealed by vital analysis. Development 122, 3929–3938.
[2] Mitchell, C.A., Risau, W. and Drexler, H.C. (1998) Regression of vessels in the tunica vasculosa lentis is initiated by coordinated endothelial apoptosis: a role for vascular endothelial growth factor as a survival factor for endothelium. Dev. Dyn. 213, 322–333.
[3] Preis, I., Langer, R., Brem, H. and Folkman, J. (1977) Inhibition of neovascularization by an extract derived from vitreous. Am. J. Ophthalmol. 84, 323–328.
[4] Felton, S.M., Brown, G.C., Felberg, N.T. and Federman, J.L. (1979) Vitreous inhibition of tumor neovascularization. Arch. Ophthalmol. 97, 1710–1713.
[5] Lutty, G.A., Thompson, D.C., Gallup, J.Y., Mello, R.J., Patz, A. and Fenselau, A. (1983) Vitreous: an inhibitor of retinal extract-induced neovascularization. Invest. Ophthalmol. Vis. Sci. 24, 52–56.
[6] Taylor, C.M. and Weiss, J.B. (1985) Partial purification of a 5.7 K glycoprotein from bovine vitreous which inhibits both angiogenesis and collagenase activity. Biochem. Biophys. Res. Commun. 133, 911–916.
[7] Zhu, M., Penfold, P.L., Madigan, M.C. and Billson, F.A. (1997) Effect of human vitreous and hyalocyte-derived factors on vascular endothelial cell growth. Aust. N. Z. J. Ophthalmol. 25 (Suppl. 1), S57–S60.
[8] Ramesh, S., Bonshek, R.E. and Bishop, P.N. (2004) Immunolocalisation of opticin in the human eye. Br. J. Ophthalmol. 88, 697–702.
[9] McMenamin, P.G., Djano, J., Wealthall, R. and Griffin, B.J. (2002) Characterization of the macrophages associated with the tunica vasculosa lentis of the rat eye. Invest. Ophthalmol. Vis. Sci. 43, 2076–2082.
[10] Lutty, G.A., Merges, C., Threlkeld, A.B., Crone, S. and McLeod, D.S. (1993) Heterogeneity in localization of isoforms of TGF-β in human retina, vitreous, and choroid. Invest. Ophthalmol. Vis. Sci. 34, 477–487.
[11] Seki, T., Yun, J. and Oh, S.P. (2003) Arterial endothelium-specific activin receptor-like kinase 1 expression suggests its role in arterialization and vascular remodeling. Circ. Res. 93, 682–689.
[12] Feng, X. and Derynck, R. (2005) Specificity and versatility in TGF-β signaling through Smads. Annu. Rev. Cell. Dev. Biol., 659–693.
[13] Goumans, M.J., Valdimarsdottir, G., Itoh, S., Rosendahl, A., Sideras, P. and ten Dijke, P. (2002) Balancing the activation state of the endothelium via two distinct TGF-β type I receptors. EMBO J. 21, 1743–1753.
[14] Oh, S.P., Seki, T., Goss, K.A., Imamura, T., Yi, Y., Donahoe, P.K., Li, L., Miyazono, K., ten Dijke, P., Kim, S. and Li, E. (2000) Activin receptor-like kinase 1 modulates transforming growth factor-β1 signaling in the regulation of angiogenesis. Proc. Natl. Acad. Sci. USA 97, 2626–2631.
[15] Kenyon, B.M., Voest, E.E., Chen, C.C., Flynn, E., Folkman, J. and D'Amato, R.J. (1996) A model of angiogenesis in the mouse cornea. Invest. Ophthalmol. Vis. Sci. 37, 1625–1632.
[16] Goumans, M.J. and Mummery, C. (2000) Functional analysis of the TGFbeta receptor/Smad pathway through gene ablation in mice. Int. J. Dev. Biol. 44, 253–265.
[17] Goumans, M.J., Lebrin, F. and Valdimarsdottir, G. (2003) Controlling the angiogenic switch: a balance between two distinct TGF-β receptor signaling pathways. Trends Cardiovasc. Med. 13, 301–307.
[18] Pepper, M.S. (1997) Transforming growth factor-beta: vasculogenesis, angiogenesis, and vessel wall integrity. Cytok. Growth Factor Rev. 8, 21–43.
[19] ten Dijke, P., Yamashita, H., Ichijo, H., Franzen, P., Laiho, M., Miyazono, K. and Heldin, C.H. (1994) Characterization of type I receptors for transforming growth factor-β and activin. Science 264, 101–104.
[20] Panchenko, M.P., Williams, M.C., Brody, J.S. and Yu, Q. (1996) Type I receptor serine-threonine kinase preferentially expressed in pulmonary blood vessels. Am. J. Physiol. 270, L547–L558.

[21] Alexander, J.M., Bikkal, H.A., Zervas, N.T., Laws Jr., E.R. and Klibanski, A. (1996) Tumor-specific expression and alternate splicing of messenger ribonucleic acid encoding activin/transforming growth factor-beta receptors in human pituitary adenomas. J. Clin. Endocrinol. Metab. 81, 783–790.
[22] Sadahira, Y., Hata, S., Sugihara, T. and Manabe, T. (1999) Bone marrow involvement in NPM-ALK-positive lymphoma: report of two cases. Pathol. Res. Pract. 195, 657–661.
[23] Coffin, C.M., Patel, A., Perkins, S., Elenitoba-Johnson, K.S., Perlman, E. and Griffin, C.A. (2001) ALK1 and p80 expression and chromosomal rearrangements involving 2p23 in inflammatory myofibroblastic tumor. Mod. Pathol. 14, 569–576.
[24] Pulford, K., Lamant, L., Morris, S.W., Butler, L.H., Wood, K.M., Stroud, D., Delsol, G. and Mason, D.Y. (1997) Detection of anaplastic lymphoma kinase (ALK) and nucleolar protein nucleophosmin (NPM)-ALK proteins in normal and neoplastic cells with the monoclonal antibody ALK1. Blood 89, 1394–1404.
[25] Johnson, D.W., Berg, J.N., Baldwin, M.A., Gallione, C.J., Marondel, I., Yoon, S.J., Stenzel, T.T., Speer, M., Pericak-Vance, M.A., Diamond, A., Guttmacher, A.E., Jackson, C.E., Attisano, L., Kucherlapati, R., Porteous, M.E. and Marchuk, D.A. (1996) Mutations in the activin receptor-like kinase 1 gene in hereditary haemorrhagic telangiectasia type 2. Nat. Genet. 13, 189–195.
[26] McAllister, K.A., Grogg, K.M., Johnson, D.W., Gallione, C.J., Baldwin, M.A., Jackson, C.E., Helmbold, E.A., Markel, D.S., McKinnon, W.C. and Murrell, J., et al. (1994) Endoglin, a TGF-β binding protein of endothelial cells, is the gene for hereditary haemorrhagic telangiectasia type 1. Nat. Genet. 8, 345–351.
[27] Srinivasan, S., Hanes, M.A., Dickens, T., Porteous, M.E., Oh, S.P., Hale, L.P. and Marchuk, D.A. (2003) A mouse model for hereditary hemorrhagic telangiectasia (HHT) type 2. Hum. Mol. Genet. 12, 473–482.
[28] Brant, A.M., Schachat, A.P. and White, R.I. (1989) Ocular manifestations in hereditary hemorrhagic telangiectasia (Rendu–Osler–Weber disease). Am. J. Ophthalmol. 107, 642–646.
[29] Vase, I. and Vase, P. (1979) Ocular lesions in hereditary haemorrhagic telangiectasia. Acta Ophthalmol. Copen. 57, 1084–1090.
[30] Mahmoud, T.H., Deramo, V.A., Kim, T. and Fekrat, S. (2002) Intraoperative choroidal hemorrhage in the Osler–Rendu–Weber syndrome. Am. J. Ophthalmol. 133, 282–284.
[31] Lamouille, S., Mallet, C., Feige, J.J. and Bailly, S. (2002) Activin receptor-like kinase 1 is implicated in the maturation phase of angiogenesis. Blood 100, 4495–4501.
[32] Roman, B.L., Pham, V.N., Lawson, N.D., Kulik, M., Childs, S., Lekven, A.C., Garrity, D.M., Moon, R.T., Fishman, M.C., Lechleider, R.J. and Weinstein, B.M. (2002) Disruption of acvrl1 increases endothelial cell number in zebrafish cranial vessels. Development 129, 3009–3019.
[33] Lebrin, F., Deckers, M., Bertolino, P. and ten Dijke, P. (2005) TGF-β receptor function in the endothelium. Cardiovasc. Res. 65, 599–608.
[34] Lebrin, F., Goumans, M.J., Jonker, L., Carvalho, R.L., Valdimarsdottir, G., Thorikay, M., Mummery, C., Arthur, H.M. and ten Dijke, P. (2004) Endoglin promotes endothelial cell proliferation and TGF-β/ALK1 signal transduction. EMBO J. 23, 4018–4028.
[35] Gabison, E., Chang, J.H., Hernández-Quintela, E., Javier, J., Lu, P.C., Ye, H., Kure, T., Kato, T. and Azar, D.T. (2004) Anti-angiogenic role of angiostatin during corneal wound healing. Exp. Eye Res. 78, 579–589.
[36] Murthy, R.C., McFarland, T.J., Yoken, J., Chen, S., Barone, C., Burke, D., Zhang, Y., Appukuttan, B. and Stout, J.T. (2003) Corneal transduction to inhibit angiogenesis and graft failure. Invest. Ophthalmol. Vis. Sci. 44, 1837–1842.
[37] Chang, J.H., Gabison, E.E., Kato, T. and Azar, D.T. (2001) Corneal neovascularization. Curr. Opin. Ophthalmol. 12, 242–249.
[38] Dawson, D.W., Volpert, O.V., Gillis, P., Crawford, S.E., Xu, H., Benedict, W. and Bouck, N.P. (1999) Pigment epithelium-derived factor: a potent inhibitor of angiogenesis. Science 285, 245–248.
[39] Chang, J.H., Javier, J.A., Chang, G.Y., Oliveira, H.B. and Azar, D.T. (2005) Functional characterization of neostatins, the MMP-derived, enzymatic cleavage products of type XVIII collagen. FEBS Lett. 579, 3601–3606.
[40] Urness, L.D., Sorensen, L.K. and Li, D.Y. (2000) Arteriovenous malformations in mice lacking activin receptor-like kinase-1. Nat. Genet. 26, 328–331.